Modeling Hydrogen Permeation through a Thin TiO_2 Film Deposited on Pd Using COMSOL Multiphysics

Z. Qin*, Y. Zeng, P.R. Norton and D.W. Shoesmith
The University of Western Ontario, London, Ontario, N6A 5B7, Canada
*Corresponding author: Department of Chemistry, The University of Western Ontario, London, Ontario, Canada N6A 5B7, zqin@uwo.ca

Abstract: Models that describe hydrogen permeation through a thin TiO_2 film deposited on Pd have been developed based on a mass-balance equation consisting of diffusion, reversible hydrogen absorption/desorption, and irreversible hydrogen trapping. These models are solved by the finite element method using COMSOL Multiphsics. By comparing model simulations with experimental permeation curves, values of the parameters associated with permeation, such as diffusion coefficients, absorption and desorption rate constants, trapping rate constants, and saturation concentrations can be evaluated. These values are required to develop models to predict hydrogen-induced cracking in oxide-covered Ti-alloys.

Keywords: hydrogen permeation, titanium oxide, palladium, thin film, model simulation

1. Introduction

Titanium and its alloys have many industrial applications thanks to their excellent corrosion resistance and high specific strength. However, they are potentially susceptible to hydrogen-induced cracking (HIC) as a consequence of hydrogen absorption.[1] Hydrogen absorbed into Ti-alloys results in the formation of hydrides and fast crack growth which ultimately could lead to failure. Generally, titanium is covered by a passive titanium oxide (TiO_2) film. Though very thin (usually a few nanometers), this compact film acts not only as a protective layer against corrosion but also as a barrier to hydrogen absorption into the metal. The impermeability of this film is, therefore, the limiting feature preventing HIC in Ti-alloys.

Hydrogen permeation through TiO_2 films is a complex process involving interfacial charge transfer, adsorption, absorption, trapping, and transport, and, thus, is inherently influenced by properties of the oxide, such as the chemical composition and structure, the presence of Ti^{n+} interstitials and/or oxygen vacancies, the type and concentration of impurities, hydrogen solubility, the adsorption characteristics of the surface, and the oxide thickness, porosity and uniformity.[2] The mechanism by which the oxide influences hydrogen permeation into Ti and its alloys is still not well established.

In aqueous solutions, measurable hydrogen absorption requires cathodic polarization leading to redox transformations within the oxide or the activation of "hydrogen windows" at defects in the film.[3] Torresi et al.[4] suggested that the activation energy for hydrogen evolution on passive titanium was much higher than on bare metal. Several studies[5,6] have shown that diffusion of hydrogen in TiO_2 is much slower than in Ti metal. Thus, the retardation of hydrogen permeation by TiO_2 films may be due to a combination of low hydrogen absorption at the oxide surface and/or slow hydrogen transport in the oxide. In general, it is difficult to predict the rate of hydrogen transport through a TiO_2 film and how many hydrogen atoms, generated on the TiO_2 surface, reach the Ti substrate.

In this communication, we present models for hydrogen permeation through a thin TiO_2 film deposited on Pd. These models are solved by the finite element method (FEM) using COMSOL Multiphysics, and compared with experimental permeation measurements.

2. Experimental

Due to complications caused by the formation of hydrides in Ti metal, a thin TiO_2 film vacuum-deposited on a Pd foil was used. Pd was selected as the substrate because of its high solubility for hydrogen and rapid kinetics for hydrogen absorption and transport.[7]

A Devanathan[8] electrochemical cell was used to measure hydrogen permeation, Figure 1. The TiO_2/Pd electrode is in the form of a membrane separating cell into two compartments. Hydrogen is generated galvanostatically on the TiO_2/solution interface by water reduction, and a fraction of the

hydrogen atoms produced are absorbed into the oxide. The hydrogen atoms then permeate through the TiO_2/Pd membrane to be re-oxidized at the Pd/solution interface at a potential at which hydrogen oxidation is diffusion controlled. The anodic currents are measured as a function of time at the Pd/solution interface yielding permeation curves presented after normalizing to the charging currents.

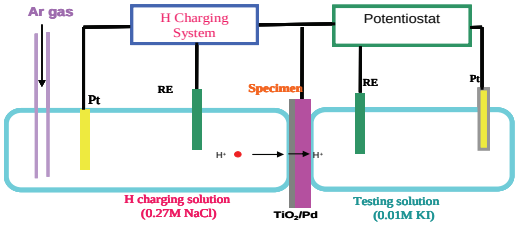

Figure 1. TiO_2/Pd electrode acting as a membrane separating the Devanathan cell into two compartments: the left side of the membrane is galvanostatically charged, and the right compartment is potentiostatically maintained at $0.18V_{SCE}$.

3. Permeation Models

Figure 2 shows schematically the processes of hydrogen permeation through a thin TiO_2 film deposited on Pd. As shown, three processes are involved, namely, (a) hydrogen diffusion, (b) reversible hydrogen absorption/desorption, and (c) irreversible hydrogen trapping.

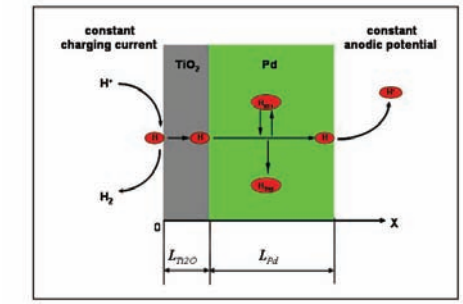

Figure 2. Schematic illustration of hydrogen permeation through a TiO_2/Pd system.

3.1 Pd Model

To investigate hydrogen permeation through oxide films on Pd, it is necessary first to clarify hydrogen permeation through Pd alone. Since the area of the Pd coupon is much greater than its thickness, a one-dimensional model is applicable. The mass balance equation accounting for the three processes is written as

$$\frac{\partial}{\partial t}C_D(x,t) = D\frac{\partial^2}{\partial x^2}C_D(x,t) - \frac{\partial}{\partial t}\left[C_A(x,t) + C_T(x,t)\right] \quad (1)$$

where C_D, C_A, and C_T are the concentrations of diffusible (free), absorbed (reversible), and trapped (irreversible) hydrogen in Pd, respectively, and D is the hydrogen diffusion coefficient. The first term on the right-hand side of Eqn (1) represents the change in the concentration as a result of diffusion, while the second represents the change due to hydrogen absorption and trapping.

The reversible absorption (hereafter referring simply as absorption) is a dynamic process in which hydrogen absorbs and desorbs. The rate equation is represented by a first-order reaction as

$$\frac{\partial}{\partial t}C_A(x,t) = k_A C_D(x,t) - k_D C_A(x,t) \quad (2)$$

where k_A and k_D are the rate constants for absorption and desorption, respectively. The trapping is an irreversible process, and its rate is assumed to be linearly proportional to the number of available trapping sites, *i.e.*

$$\frac{\partial}{\partial t}C_T(x,t) = k_T\left(1 - \frac{C_T(x,t)}{C_T^S}\right)C_D(x,t) \quad (3)$$

where k_T is the trapping rate constant, and C_T^S is the saturation concentration of trapped hydrogen.

The two surfaces of the Pd coupon are galvanostatically or potentiostatically controlled, yielding the boundary conditions,

$$-D\frac{\partial}{\partial x}C_D(x=0,t) = f_H\frac{i_0}{F} \quad (4)$$
$$C_D(x=L,t) = 0$$

where i_0 is the charging current density, f_H is the charging efficiency defined as the ratio of the

hydrogen produced to that absorbed by the oxide, F is the Faraday constant, and L is the thickness of the Pd coupon. Initially, the coupon is free of hydrogen, *i.e.*

$$C_D(x,t=0) = C_A(x,t=0) = C_T(x,t=0) = 0 \qquad (5)$$

Once steady state is established, the charging current is turned off, and the hydrogen absorbed during charging begins to be released. During this discharge period, the mass balance is governed by

$$\frac{\partial}{\partial t}C_D(x,t) = D\frac{\partial^2}{\partial x^2}C_D(x,t) - \left[k_A C_D(x,t) - k_D C_A(x,t)\right] \qquad (6)$$

Eqn (6) does not contain a trapping term because this process is irreversible, and does not occur after all available sites have been saturated. During a discharging period, the hydrogen will be released from both sides of the Pd coupon under the conditions,

$$C_D(x=0,t>t_0) = C_D(x=L,t>t_0) = 0 \qquad (7)$$

where t_0 is the charging time.

3.2 TiO_2/Pd Model

For simulations depending on meshing, such as FEM, difficulties are often encountered in models containing thin layers since large geometric scale variations are present (in the present case 24nm:0.1mm). Three approaches have been attempted. The first approach used actual dimensions but different mesh densities in the TiO_2 and Pd. Simulations appeared to yield reasonable results on certain parameter values but not on others. The second approach used different length scales in the TiO_2 and Pd subdomains, with the diffusion and absorption parameters normalized accordingly. However, normalization of the flux is ambiguous at TiO_2/Pd interface. To overcome this difficulty due to the large differences in dimensions of the TiO_2 film and Pd, the thin-layer approximation was applied, in which the thin TiO_2 film is replaced by a boundary layer sandwiched between a hypothetical fast diffusion layer (FDL) and the Pd, as demonstrated in Figure 3.

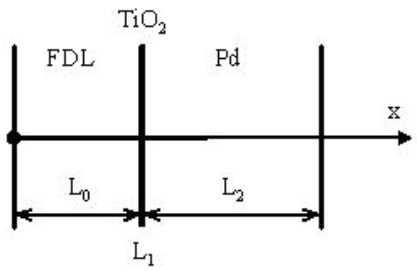

Figure 3.Schematic illustrating the sandwich model in which the TiO_2 film is represented as a boundary layer between a fast diffusion layer (FDL) and the Pd

The FDL is a hypothetical layer in which diffusion is so fast that it has a little effect on the subsequent TiO_2 and Pd, as given by

$$\frac{\partial}{\partial t}C_0(x,t) = D_0\frac{\partial^2}{\partial x^2}C_0(x,t) \qquad (D_0 >> D_1, D_2) \qquad (8)$$

Hereafter we use subscripts '0', '1' and '2' referring to diffusional quantities in the FDL, TiO_2 and Pd, respectively.

Absorption and trapping are negligible in TiO_2 since it is very thin. Diffusion in TiO_2 is not explicitly treated, but incorporated as interior boundary conditions in the sandwich model. The flux at the interior boundary is approximated by the equation,

$$J_1(t) = -\frac{D_1}{L_1}\left(C_2(L_0^+,t) - C_0(L_0^-,t)\right) \qquad (9)$$

where $C_0(L_0^-,t)$ and $C_2(L_0^+,t)$ are the concentrations at the left and right surfaces of the boundary layer, and D_1 and L_1 are the hydrogen diffusion coefficient and thickness of the TiO_2 layer, respectively. At the interior boundary the concentrations are discontinuous, and can be calculated using the assembly feature. A similar approach has been applied in modeling contact resistances between metals.[9] The Pd is still governed by Eqns (1)–(3), and the boundary conditions at the entrance and exit are as stated in Eqn (4).

After charging for a period of time, a steady state is achieved at which all concentrations are time-independent. At steady state, these concentrations can be determined analytically as

$$C_0^{ss}(x) = \frac{f_H i_0}{F \cdot D_0}(L_0 - x) + \frac{f_H i_0}{F}\left(\frac{L_1}{D_1} + \frac{L_2}{D_2}\right)$$
$$C_2^{ss}(x) = \frac{f_H i_0}{F \cdot D_2}(L_0 + L_2 - x) \qquad (10)$$
$$C_A^{ss}(x) = \frac{k_A}{k_D} C_2^{ss}(x); \quad C_T^{ss}(x) = C_T^S$$

where C_0^{ss} is the steady state hydrogen concentration in the FDL, and C_2^{ss}, C_A^{ss}, and C_T^{ss} are the steady state concentrations of diffusible, absorbed, and trapped hydrogen in Pd, respectively. Once steady state is established, the charging current is turned off. During a discharging period, though very thin, the TiO_2 film acts as a barrier that blocks hydrogen release from the TiO_2/Pd side. Therefore the boundary conditions during discharge are given by

$$D_1 \frac{\partial}{\partial x} C_1(x = L_0, t > t_0) = 0 \qquad (11)$$
$$C_2(x = L_0 + L_2, t > t_0) = 0$$

4. Results and Discussion

The permeation models developed in Section 3 were simulated by COMSOL Multiphysics (Chemical Engineering Module, version 3.4), and compared with experimental permeation curves. This procedure was first applied to a Pd-only system to obtain the permeation parameters in Pd, and then extended to the TiO_2/Pd system to derive the parameters for the TiO_2 film. The values of simulation parameters are tabulated in the Appendix.

Figure 4 shows the permeation curves measured in Pd when charging at 80 nA/cm^2. The curves show some features typically observed in transport-absorption processes.[10] After a time lag, the permeation current increases, initially rapidly, before more slowly achieving the steady-state value from which the charging efficiency f_H can be calculated. Once the charging current is switched off, the permeation current drops, but not immediately back to a background value, with the tailing off as a consequence of the release of the hydrogen absorbed during charging.

The model simulation fits the experimental result well, indicating that the model is a reasonable description of the permeation process. The diffusion coefficient obtained from the simulation, 3.34×10^{-7} cm^2/s, is consistent with published values.[7,11] No published data are available for comparison to the absorption/desorption rate constants, the trapping rate constant, and the trapping saturation in Pd. The ratio k_A/k_D = 80 indicates that the reversible absorption process is only slightly reversible, and may not be easily separable from the irreversible trapping process. The values of k_A and k_D were thus calculated from the discharging period where only reversible absorption is active. The values of k_T and C_T^S indicate that the Pd specimens have a number of traps that strongly interact with hydrogen. One possible source for such traps is the cold-working of the Pd foils during fabrication.

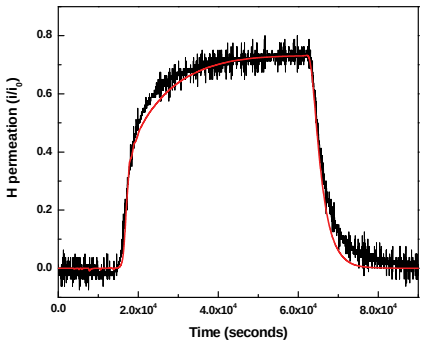

Figure 4. A model simulation (—) compared to an experimental permeation curve (—) obtained for Pd

The experimental and simulated permeation curves for TiO_2/Pd charging at 80 nA/cm^2 are shown in Figure 5. For Pd, the parameter values obtained for the Pd-only simulations were applied, on the assumption that the properties of the Pd are uninfluenced by the TiO_2 layer. The model simulation reproduces the experimental permeation curve over the charging period, but a notable discrepancy is observed over the discharge period. During discharge, the TiO_2 film acts as a barrier to hydrogen release, allowing hydrogen release only from one side (*c.f.* Eqns (7) and (11)). Hence, discharge would be expected to be slower for TiO_2-covered Pd than for bare Pd. The observed steep decrease without tailing cannot presently be explained, and requires further investigation.

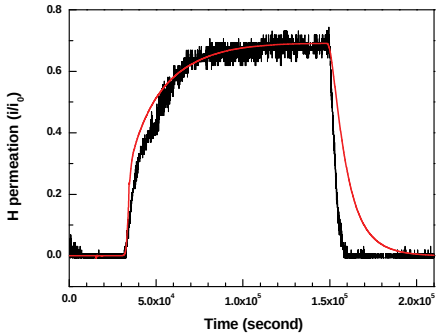

Figure 5. A model simulation (—) compared to an experimental permeation curve (—) for TiO_2 deposited on Pd

Comparison to the Pd-only system shows that the TiO_2 film noticeably impedes hydrogen permeation. The charging efficiency for TiO_2/Pd (0.6935) is smaller than that for Pd (0.7325), indicating that a smaller fraction of the hydrogen produced on a TiO_2 surface is absorbed compared to that absorbed on a bare Pd surface. However, the most remarkable effect is in the times required for permeation currents to start rising and to achieve the steady state, which are doubled for TiO_2/Pd compared to Pd. This could suggest that hydrogen transport through the oxide rather than hydrogen evolution at the oxide surface is responsible for the strong retardation of TiO_2 films on hydrogen permeation.

The hydrogen diffusion coefficient in TiO_2 films, D_1, is one of the most important parameters in predicting HIC in Ti-alloys. The value of D_1 obtained in this study (10^{-13} cm^2/s) is three orders of magnitude lower than that in Ti metal,[12] and close to that found by Pyun et al.[5] ($(3.9\text{-}5.2)\times10^{-14}$ cm^2/s), but higher than that obtained by Pound[4] (7.5×10^{-20} cm^2/s) in TiO_2. The D_1 calculated by the present models can be regarded as an apparent or effective diffusion coefficient, which includes the influence of absorption and trapping in the oxide.

Figure 6 shows the simulation results for various values of D_1, and demonstrates that hydrogen permeation is very sensitive to hydrogen diffusion in the oxide. The slower the diffusion through TiO_2, the longer the time-lag before permeation commences, and the longer the time required to achieve steady state. Figure 6 also confirms that 10^{-13} cm^2/s is an optimized value in fitting the experimental data.

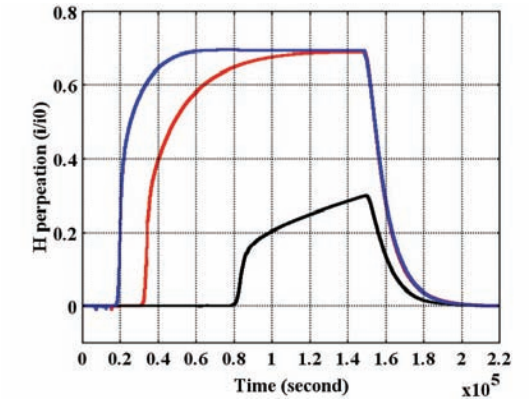

Figure 6. Effect of diffusion in TiO_2 on permeation curves: (—) $D_1 = 10^{-16}$ m^2/s, (—) $D_1 = 10^{-17}$ m^2/s, (—) $D_1 = 10^{-18}$ m^2/s (other simulation parameters are shown in Table 1)

5. Conclusions

Models describing hydrogen permeation through a thin TiO_2 film deposited on Pd were developed and solved using COMSOL Multiphysics. Comparison of simulated and experimental permeation curves shows the models provide a better understanding of the mechanistic details of hydrogen absorption by oxide-covered Ti and yields values of the permeation parameters required to predict HIC in Ti-alloys. While focused specifically on the TiO_2/Pd system, the models can be readily adapted to other material systems.

6. References

1. Z. Qin and D.W. Shoesmith, Failure model and Monte Carlo simulations for titanium (Grade-7) drip shields under Yucca mountain repository conditions, *J. Nuclear Materials*, **379**, 169-173 (2008)

2. B. Pound, Hydrogen ingress during corrosion, *Corrosion and Oxide Films*, 118-155, WILEY-VCH (2003)

3. F. Hua, K. Mon, P. Pasupathi, G. Gordon, D. W. Shoesmith, A review of corrosion of titanium grade 7 and other titanium alloys in nuclear waste repository environments, *Corrosion*, **61**, 987-1003 (2005)

4. R.M. Torresi, O.R. Camara, C.P. De Pauli, and M.C.Giordano, Hydrogen evolution reaction on anodic titanium oxide films, *Electrochimca Acta*, **32,** 1291-1301 (1987)
5. B.G. Pound, Hydrogen ingress in titanium, *Corrosion*, **47**, 99-104 (1991)
6. S. Pyun, J. Park, and Y. Yoon, Hydrogen permeation through PECVD (plasma-enhanced chemical vapor deposition) TiO_2 film on Pd by the time lag method, *J. Alloys and Compounds*, **231**, 315-320 (1995)
7. S.I. Pyun and Y.G. Yoon, Hydrogen transport through metals determined by electrochemical methods, *International Materials Reviews* **45**, 190-216 (2000)
8. M.A.V. Devanathan and Z. Stachrski, The adsorption and diffusion of electrolytic hydrogen in palladium, *Proc. Roy. Soc.*, **270,** 90-102 (1962)
9. Thin film approximation: contact resistance, *COMSOL Support Knowledge Base* No. 902 (2008)
10. Z. Qin, J.C. Wren, and C.J. Moore, Modeling the iodine removal efficiency and temperature behavior for an FADS charcoal filter by FEMLAB, *Proc. FEMLAB Conf. (Boston, MA, Oct. 23-25, 2005)*, edited by J. Hiller, 119-123 (2005)
11. C. Gabrielli, P.P. Grand, A. Lasia, and H. Perrot, Investigation of hydrogen adsorption and absorption in palladium thin films III: Impedance spectroscopy, *J. Electrochem. Soc.* **151**, A1943-A1949 (2004)
12. P.A. Sundaram, E. Wessel, H. Clemens, H. Kestler, P.J. Ennis, W.J. Quadakkers, L. Singheiser, Determination of the diffusion coefficient of hydrogen in gamma titanium aluminides during electrolytic charging, *Acta Materialia*, **48**, 1005-1019 (2000)

7. Acknowledgements

This work was supported by National Science & Engineering Research Council of Canada.

8. Appendix

Table 1: Values of simulation parameters

	Value	Description
i_0	8×10^{-4} A/m^2	charging current density
f_H	0.6935	charging efficiency
t_0	149000 s	charging time
L_0	1×10^{-5} m	FDL thickness
L_1	2.4×10^{-8} m	TiO_2 thickness
L_2	0.0001 m	Pd thickness
D_0	1×10^{-5} m^2/s	diffusion coefficient in FDL
D_1	1×10^{-17} m^2/s	diffusion coefficient in TiO_2
D_2	3.34×10^{-11} m^2/s	diffusion coefficient in Pd
k_A	1 s^{-1}	absorption rate constant in Pd
k_D	0.0125 s^{-1}	desorption rate constant in Pd
k_T	10 s^{-1}	trapping rate constant in Pd
C_T^S	0.58 mol/m^3	trapping saturation in Pd